

Received 24 October 2023, accepted 11 November 2023, date of publication 14 November 2023, date of current version 22 November 2023.

Digital Object Identifier 10.1109/ACCESS.2023.3332666

## RESEARCH ARTICLE

# Mountain Gazelle Algorithm-Based Optimal Control Strategy for Improving LVRT Capability of Grid-Tied Wind Power Stations

FATMA EL ZAHRAA MAGDY<sup>1</sup>, HANY M. HASANIEN<sup>1,2</sup>, (Senior Member, IEEE),  
WAHEED SABRY<sup>3,4</sup>, ZIA ULLAH<sup>5</sup>, (Member, IEEE),  
ABDULAZIZ ALKUHALI<sup>6</sup>, (Member, IEEE), AND AHMED H. YAKOUT<sup>1</sup>

<sup>1</sup>Department of Electrical Power and Machines, Faculty of Engineering, Ain Shams University, Cairo 11517, Egypt

<sup>2</sup>Faculty of Engineering and Technology, Future University in Egypt, Cairo 11835, Egypt

<sup>3</sup>Giza Engineering Institute, Cairo 12511, Egypt

<sup>4</sup>Military Technical College (MTC), Cairo 11528, Egypt

<sup>5</sup>School of Electrical and Electronic Engineering, Huazhong University of Science and Technology, Wuhan 430074, China

<sup>6</sup>Department of Electrical Engineering, College of Engineering, King Saud University, Riyadh 11421, Saudi Arabia

Corresponding author: Hany M. Hasanien (hanyhasanien@ieee.org)

This work was supported by the King Saud University, Riyadh, Saudi Arabia, through the Researchers Supporting Project under Grant RSP2023R258.

**ABSTRACT** The large-scale wind energy conversion systems (WECS) based on a doubly fed induction generator (DFIG) have recently gained attention due to their numerous economic and technological advantages. However, the rapid integration of WECS with standing power networks severely influenced the system's reliability and stability; also, the DFIG rotor circuit experiences a substantial overcurrent due to grid voltage fluctuations. Indeed, these problems emphasize the significance of a DFIG's low-voltage ride-through (LVRT) capacity in maintaining the stability of the electrical grid during voltage fluctuations. To solve these challenges simultaneously, this research employs a metaheuristic optimization technique to regulate a doubly fed induction generator's (DFIG) operation via a wind turbine (WT) system. The article proposes a novel Mountain Gazelle Optimizer (MGO) to optimize the proportional-integral (PI) controller gains for the DFIG system's active and reactive power control to enhance the LVRT capability of Wind turbines linked to the power grid. In the proposed scheme, LVRT improvement is proportional to undershoot or overshoot, settlement time, and steady-state inaccuracy of voltage responses. The proposed control method is implemented in MATLAB by a detailed model of 9MW wind turbine, and its performance is validated and compared with traditional optimization control approaches. The suggested MGO method's efficacy is demonstrated by the assessment and comparison to classic optimization-based PI controllers under various fault scenarios. The simulation results show that the optimized control method improved performance in terms of three-phase terminal voltage output responses, active power, reactive power demand to networks, and DC-Link voltage.

**INDEX TERMS** Doubly fed induction generator, low-voltage ride-through capability, metaheuristic optimization, mountain gazelle optimizer, wind energy conversion systems.

## I. INTRODUCTION

### A. OVERVIEW

This The integration of renewable energy sources into the electric grid is gaining popularity due to its sustainability and

The associate editor coordinating the review of this manuscript and approving it for publication was Youngjin Kim<sup>1</sup>.

techno-economic benefits. In particular, solar and wind power have become the fastest-growing sources of new electric generation in recent years, and their costs have been declining rapidly. However, the intermittency of these renewable energy sources (RESs) presents a challenge to their integration into the power grid and networks; they face significant challenges related to grid stability and reliability, particularly during grid

disturbances. One of the key concerns in this context is the Low Voltage Ride Through (LVRT) capability of grid-tied wind power stations. Ensuring a high LVRT capability is essential for minimizing power supply interruptions, enhancing grid stability, and preventing costly equipment damage. Energy storage technologies such as batteries, pumps for storing water, and thermal storage are being developed and deployed to address the challenges of intermittency. Worldwide, governments are applying development programs that encourage the usage of energy from RESs and minimize reliance on fossil fuels. This includes feed-in tariffs, tax credits, and renewable portfolio standards. Private sector companies are also investing in renewable energy projects and setting targets for using renewable energy [1], [2], [3]. The tactical goals of Egypt's New and Renewable Energy Authority (NREA), endorsed around 2008, intend to use renewable energy sources to produce 20% of all power by today (2023), with wind energy sources (WES) accounting for 12% of the total [4], [5]. A DFIG is currently mainly widely utilized in wind power plants, given its particular features such as changing speeds, real-time management of power, and steady frequency. In addition, minimal-rated light converters for power are used, which have fewer losses and less of an influence on gears [6], [7]. DFIG turbines are more utilized in power systems cause of their direct net connectivity and because of the lower cost of the converter that processes the slip power over the rotor side [8]. Moreover, it's worth mentioning that the DC-link's capacitor or rotor both risk overheating due to the sudden voltage drop. The power converters deteriorate and may potentially fail without protection. The turbine's capacity for proper functioning deteriorates, causing it to be disconnected from the network [9]. Hence, low-voltage ride-through capability (LVRT) must be improved to develop this DFIG functionality [10], [11].

## B. RESEARCH MOTIVATION

Many important factors necessitate further investigation into appropriate control strategies for improving the LVRT capacity of grid-connected wind power facilities. Firstly, with the escalating global emphasis on clean energy sources, wind power has emerged as a crucial component in achieving sustainable and low-carbon electricity generation. Nevertheless, wind turbines are particularly susceptible to voltage dips and grid disturbances, exposing their reliability and the stability of the power grid. This research is motivated by the imperative to develop advanced control methodologies that empower wind power stations to navigate these challenges effectively, ensuring their continuous operation during voltage fluctuations and protecting the grid against potential disruptions. Furthermore, as regulatory entities and industry standards continue to grow, stringent requirements for LVRT performance have been established to maintain grid operation and resilience. Moreover, the adapted research focuses on grid resilience, as generally, the power systems experience grid disturbances like faults or short circuits; these disturbances

can cause voltage dips, which can disrupt power supplies if wind power stations are unable to ride through these events, it can result in substantial power supply disruptions. Enhancing LVRT capability is crucial for maintaining grid resilience and minimizing downtime. Also, renewable energy integration into the system is more challenging than integrating wind power generation. Hence, to operate smoothly and stabilize the grid, grid-tied wind power stations need advanced control systems. In addition, regulatory organizations and industry standards have evolved, resulting in strict criteria for LVRT performance to preserve grid integrity and resilience.

Furthermore, as regulatory bodies and industry standards continue to evolve, stringent requirements for LVRT performance have been established to maintain grid integrity and resilience. Adhering to these standards is not only a regulatory necessity but also a strategic imperative for power generation companies. Non-compliance can lead to consequences, operational limitations, and reputational risks. Thus, this research is motivated by the need to create an appropriate control solution that not only meets existing LVRT standards but also proactively anticipates wind power integration. By addressing these essential challenges, this research aims to advance the capabilities of grid-tied wind power stations, bolster grid stability, and ultimately contribute to a more reliable, sustainable, and environmentally responsible energy landscape.

## C. LITERATURE REVIEW

LVRT capability refers to a WT's ability to retain its voltage when a fault occurs in the grid [12]. However, network coding requires that turbines be connected to the system in voltage dip conditions up to a particular degree to support the network. By controlling reactive and active electrical power and protecting its power converters, efficient LVRT schemes are essential for grid system support. According to several surveys, pitch control techniques, improved hardware methods, and enhanced DFIG converter control approaches contribute to improving the LVRT schemes [13]. By adjusting the rotor blades' pitch angle with pitch control, the turbine's power performance can be reduced. This approach, however, performs poorly because of the sluggish mechanical blade system [14]. The primary hardware techniques for LVRT enhancement are crowbar protection and energy storage systems [15], [16]. In the event of a failure, the crowbar technique connects resistor banks in the DFIG rotors circuit, causing an increase in power losses restricting DFIG electrical currents. Furthermore, this approach has numerous flaws, including increased drive train stress caused by magnetic torque changes, control damage, and network voltage restoration inhibition owing to reactive energy absorption. Other hardware approaches for improving LVRT include using energy storage systems, such as battery-powered energy storage systems, electromagnetic flywheel vitality storing systems, electrically powered double-layer capacitors, or superconductor magnets [17], [18]. However, the main disadvantage of this strategy is that

it is not a cost-effective option. Due to the drawbacks of pitch control and the high cost of energy storage systems, papers have been looking into using the DFIG converter control to improve the DFIG -LVRT capability for its simplicity, minor expenses, and quick control [19], [20]. The selection and optimization of PI controller gains utilized to extract stator and rotor variable references are vital to the method's efficiency [21], [22].

For example, it was first suggested to utilize Particle Swarm Optimization (PSO) for optimizing converter controller gains [23], [24]. However, the ordinary PSO will eventually reach a global minimum, but No assurance is given that it will be helpful for all controller design challenges. For minor and significant conflicts, Controllers for PI with PSO optimization result in considerable damping plus high overshoot [25]. Although It converges quickly, it has poor accuracy [26], [27]. Wang et al. [28] compared both PSO and Bacteria Foraging Optimization (BFO), and PSO produced better results than (BFO). Regarding settling and rising time, Zhu et al. [29] utilized the Bat Algorithm (BA) optimized sliding mode controller, which outperforms both the PI controller tuning and the standard sliding mode controller. However, there was some inconsistency in the voltage amplitude of the stator side. BA has a quick convergence time but poor accuracy [30]. Hongwei et al. [31] compared the genetic algorithm (GA) with the moth flame optimization (MFO). A tuned ideal PI controller based on Moth Flame Optimization (MFO) was found to improve LVRT. It considers the use of excellent selection capabilities; however, its slow rate of conversations causes it to become stranded in the local optimal conditions.

Krause et al. [32] presented a PI controller for a wind farm with permanent-magnetic synchronous generators developed with the Golden Eagle Optimization [GEO] algorithm, which was determined to be superior to GA, PSO, and Newton Rapson [NR] in terms of strategy and efficiency. The GEO is utilized to adjust the gain setting of the PI controls of the rotors in addition to grid-side converters (RSC and GSC). Controllers were tuned using the GEO method during transient and dynamic analysis. Under variable wind conditions, the GEO can gather the maximum wind power while improving LVRT [33]. Abdelateef Mostafa et al. [34] Utilized The bonobo optimization method (BO), which was compared to two additional Techniques, PSO and the Driving train algorithm (DTA). The three optimization techniques produced remarkably similar findings.

Yamparala et al. [35] introduced optimal controller parameter selection with a hybrid algorithm that combines the sea lion and grey wolf (SLNO+GWO). The previous optimization technique was used to design a fractional-order PID controller (FOPID) and compared it to Root tree-optimized PI controllers (RTO+PI). Results show a reduction of reactive and active powers. Moreover, the DC link Harmonic currents were stabilized and reduced by 2.56%. Concerning nonlinear control theory considerations, Tilli et al. [36]

presented a unique control modification for back-to-back converters to avoid rotational converter tripping, and this suggested approach uses mixed feedback and feedforward terms. The proposed method has the benefits of being strong and providing extra oscillation damping. Mosaad et al. [37] introduced an integrated model of a PI-based controller to enhance DFIG's LVRT capacity via wind-power technology. This crossbred approach associations random-forest and elephant herd methods. The improved elephant herd method, which takes into account several LVRT parameters such as voltage, current, and active in addition to reactive power, identifies the outstanding choices from the accessible Offline space exploration as well as dataset creation. Hiremath et al. [38] presented an improved super-twist method for LVRT enhancement at different voltage drop conditions. Under transient circumstances, the suggested technique enhanced LVRT capabilities in the case of particular wind turbine systems besides real wind farms.

Scientists have been developing new optimization techniques to overcome the disadvantages of all previously mentioned optimization techniques. A recent optimization technique that has proven to be robust and fast in convergence is the mountain gazelle optimization (MGO). MGO is an algorithm that takes inspiration from wildlife and emulates hunting and prey selection procedures in the wild. The global optima are readily identified using a statistical representation of the searching trajectory. Hence, this paper tests and uses the novel technique to optimize rotor and grid side converters PI controllers and contrast the outcomes with different optimization techniques, specifically PSO and GA. The main contributions of this paper can be summarized as follows:

- A new optimization technique is applied to optimize the PI controllers' gains and LVRT capabilities of DFIG wind farms: Mountain Gazelle Optimize (MGO).
- The optimal control system's effectiveness is demonstrated by comparing simulation results to other conventional optimization-based PI controllers like genetic algorithm (GA) and particle swarm optimization (PSO) methods.
- To validate the proposed control method, a system with the optimal recommended control technique is evaluated in various fault situations (symmetrical and unsymmetrical) to test the authority technique thoroughly.

This paper has the following structure: Section I serves as an introduction. The modeling and operating model of DFIG and the problem formulation are recognized in Section II. The recommended techniques and algorithms used to optimize the PI converter controllers, such as the MGO method and its theory, are presented in Section III. Moreover, the DFIG system Simulink response and comparative analysis of the time domain for MGO, PSO, and GA-based controllers are presented in Section IV. Finally, conclusions and short deliberations are deliberated in Section V.

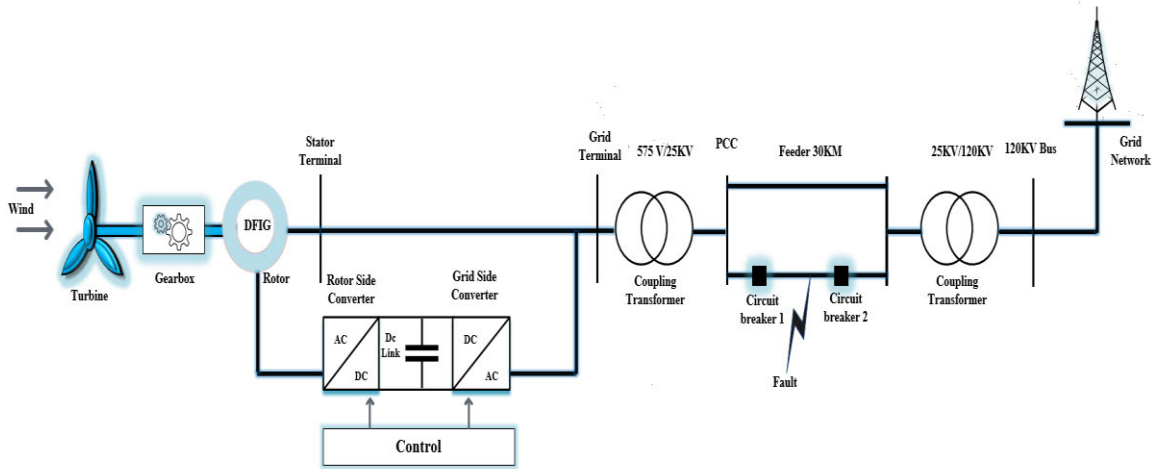


FIGURE 1. Single line diagram for grid-connected DFIG-WT.

II. DYNAMIC MODELING OF WIND STATION

The case studied in this paper is a VSWT- DFIG connected to the electrical grid through wind farms by two feeders. The proposed wind farm being considered has six 1.5 MW WTs, generating 9 MW. The wind farm is coupled with a 25 kV delivery scheme that carries 120 kV electrical power to the network throughout a 30 km transmission Line through two 25 kV feeders. The DFIG system and its control are addressed deeply in the following subsections. Moreover, Figure 1 shows the DFIG system’s single-line diagram.

A. VSWT MODELLING

The relationship below illustrates how the wind turbine generators’ mechanical power  $P_m$  is represented [1].

$$P_m = 0.5 \cdot \rho \cdot A \cdot V^3 \cdot C_p(\lambda, \beta) \tag{1}$$

In Eq. (1),  $P_m$  represents the aerodynamic power of the WT, which is a function of multiple variables, for example, The density of air ( $\rho$ ), rotor swept area ( $A$ ), wind speed ( $V$ ), coefficient of powers ( $C_p$ ), which in turn, depends on the speed ratio of the tips ( $\lambda$ ) and the pitched angle of the blade ( $\beta$ ). The expression for  $P_m$  in Eq. (1) shows that the power output of the WT rises with the cube of wind velocity, as well as proportional to the rotor’s swept area and the density of air. The power coefficient ( $C_p$ ), gauges WT’s effectiveness in extracting power from the wind, is determined using the speed ratio and the blades’ pitch angle. A blade’s tip speed ratio is defined as the ratio of the tangential speed of the blade tip to the speed of the wind, and the blade pitch angle is the angle formed between the length of the blade and its plane of rotation. Equation (1) is often utilized in WT assessment and implementation to estimate power production under different operating conditions [1].

Equation (2) gives the expression for  $C_p$ , which depends on  $\lambda$  and  $\beta$ . The element  $\gamma$  is reliant on  $\lambda$  and  $\beta$ , and is

specified by

$$C_p(\lambda, \beta) = 0.22 \left( \frac{116}{\gamma} - 0.4\beta - 5 \right) \cdot \exp\left( \frac{-12.5}{\gamma} \right) \tag{2}$$

Equation (3).  $C_p$  denotes the WT’s efficiency in transforming power from wind to mechanical power.

$$\frac{1}{\gamma} = \frac{1}{\lambda + 0.089} - \frac{0.035}{\beta^3 + 1} \tag{3}$$

$\lambda$  is described as a relationship between wind speed and blade tip speed. It is a significant measurement in WT design and operation because it marks the aerodynamics of the turbine’s effectiveness and effectiveness.  $\lambda$  is influenced by the rotor’s radius ( $R$ ) plus angular velocity ( $\omega$ ) as presented in Equation (4).

$$\lambda = \frac{R \cdot \omega}{V} \tag{4}$$

Because of the presence of a gearbox with a gear ratio ( $N_{gb}$ ), the dynamic model wind turbine angular velocity ( $\omega$ ) is related with the rotor speed ( $\omega_{optimum}$ ) as explained below in Equation (5).

$$\omega = N_{gb} * \omega_{optimum} \tag{5}$$

The formula for the torque acting on the shaft (mechanical torque) of wind turbines ( $T_m$ ) is specified by Equation (6), which is developed from the mechanical power equation that links the mechanical power generated by the turbine to the rotational blades’ speed. As for  $C_p$  It shows how effectively the WT converts the kinetic energy from wind into mechanical energy. It achieves its peak at the ideal tip speed ratios [39].

$$T_m = \frac{P_m}{\omega} \tag{6}$$

**B. DFIG MODELING**

As indicated in Figure 1, Energy converters provide electricity to the rotor terminals straight-linked to the network by the DFIG stator terminals. At a steady state, the converter on the rotor side independently regulates the stator’s reactive and active energy. At the same time, the voltage throughout the direct current link is kept constant by the net side converter. Within a coordinate system called *dq*-coordinates, a generator model is constructed [40]. Both rotor and stator voltage formulas, as well as the flux factors, are shown below from equations (7)-(10).

$$V_{ds} = R_s \cdot I_{ds} + \frac{d\phi_{ds}}{dt} - \omega_s \phi_{qs}$$

$$\phi_{qs} = L_s I_{qs} + L_m I_{qr}$$
(7)

$$V_{qs} = R_s \cdot I_{qs} + \frac{d\phi_{qs}}{dt} - \omega_s \phi_{ds}$$

$$\phi_{ds} = L_s I_{ds} + L_m I_{dr}$$
(8)

$$V_{dr} = R_r \cdot I_{dr} + \frac{d\phi_{dr}}{dt} - (\omega_s - \omega_r) \phi_{qr}$$

$$\phi_{qr} = L_r I_{qr} + L_m I_{qs}$$
(9)

$$V_{qr} = R_r \cdot I_{qr} + \frac{d\phi_{qr}}{dt} - (\omega_s - \omega_r) \phi_{dr}$$

$$\phi_{dr} = L_r I_{dr} + L_m I_{ds}$$
(10)

The formula of voltage equations in coordinates depends on ( $\omega_r, \omega_s$ ) are Rotor and Stator Frequency, ( $R_s, R_r$ ) are Rotor and Stator Resistance,  $L_m$  is Magnetizing Inductance, ( $L_s, L_r$ ) Stator and rotor Winding Leakage Inductances ( $I_{ds}, I_{qs}, I_{dr}, I_{qr},$ ) are stator and rotor current, flux components are all in the *d-q* reference as ( $\phi_{qs}, \phi_{ds}, \phi_{qr}, \phi_{dr}$ ) are connected to the same frame [40].

The Equation of the electromagnetic torque is:

$$T_e = -\frac{3}{2} p \frac{L_m}{L_s} (\phi_{ds} I_{qr} - \phi_{qs} I_{ds})$$
(11)

where *p* is the number pair of poles.

**C. DFIG ACTIVE IN ADDITION TO REACTIVE POWER CONTROL**

The control unit of the rotor side (RSC) scheme of DFIG is shown in Figure 2. It utilizes the rotational currents along the *q* and *d* axes,  $i_{qr}$  and  $i_{dr}$ , to regulate the reactive and active powers of the stator ( $P_s, Q_s$ ). The stator’s output power is obtained using the wind system’s maximum power (MPPT). By employing MPPT, the turbine continuously operates at its maximum power, optimizing generating wind electricity. On the other hand, control on the grid side (GSC) is demonstrated in Figure 3. It regulates the voltage level at the DC connection and the rate of reactive power exchanges in a point of communal coupling (PCC). Using the alternating current (AC) references frames in line with the wind turbine’s rotor circuit’s flow of energy direction. The PCC is the point where a wind turbine is linked to the power network [41], [42].

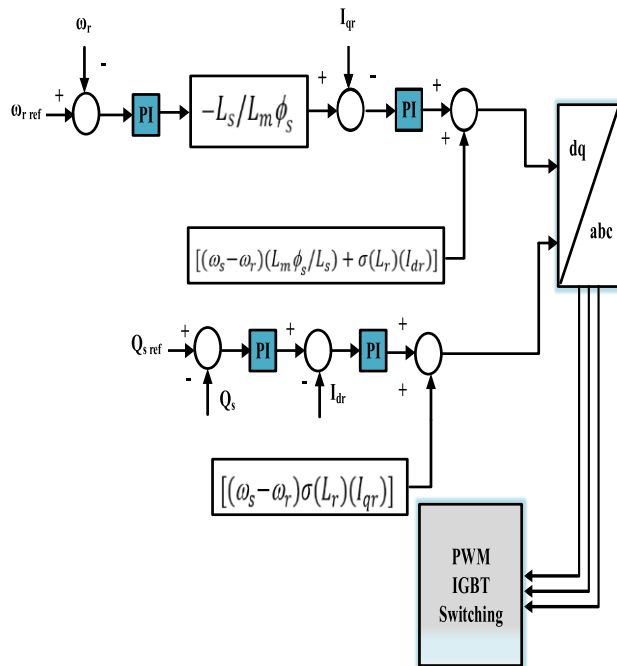


FIGURE 2. DFIG RSC control circuit.

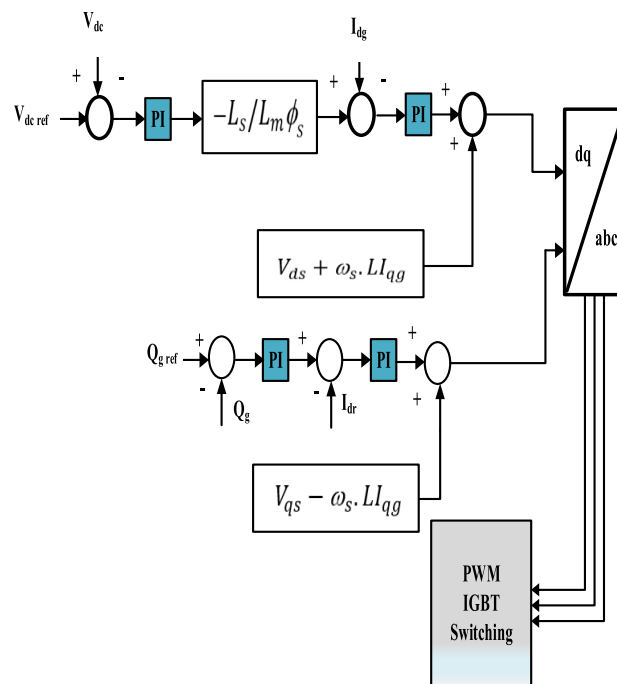


FIGURE 3. DFIG GSC control circuit.

The reactive, as well as the active power of the stator is provided by [43] and [44]:

$$P_s = V_{ds} I_{ds} + V_{qs} I_{qs} = -V_s \frac{L_m}{L_s} I_{qr}$$

$$Q_s = V_{qs} I_{ds} - V_{ds} I_{qs} = -V_s \frac{L_m}{L_s} I_{dr} + V_s \frac{\phi_s}{L_s}$$
(12)

Wherever: ( $V_s$ ) is Stator Voltage and ( $\phi_s$ ) is Stator flux.

**D. PROBLEM FORMULATION**

In our study, we optimize the gains of controllers in the rotor and grid side’s outer loop, which are [k<sub>p</sub>\_Rotor side current regulator, k<sub>i</sub>\_Rotor side current regulator, k<sub>p</sub>\_Voltage regulator, k<sub>i</sub>\_Voltage regulator, k<sub>p</sub>\_Dc bus regulator, k<sub>i</sub>\_Dc bus regulator, k<sub>p</sub>\_grid side current regulator, k<sub>i</sub>\_Grid side current regulator]. The objective function considered is the integral time absolute error (ITAE) of the DFIG terminal voltage. This criterion is used for its popularity in improving system dynamics. Moreover, Table (1) shows the optimization algorithm parameters and constraints. Equation (13) expresses the ITAE index as such. This study evaluates the PI controller using a time domain criterion.

$$ITAE = \int_{t=0}^{t=final} |\Delta v| * t * dt \quad (13)$$

**TABLE 1. Model parameters constraints.**

The Optimizer's Name	Parameters	Ranges
MGO PSO GA	Maximum Number of Iterations	25
	Size of Population	30
	Lower Bound of Variables	1
	Upper Bound of Variables	200
	Number of Decision Variables	8

**III. TECHNIQUES AND ALGORITHMS**

The mountain gazelle optimization technique is a novel method used in case studies from the real world. This approach may be utilized to solve challenges involving multiple objectives. This Metaheuristic method is employed in a wide variety of problems.; it can be used to address recombination optimization problems and diversified problems with various anchors and, according to that, applied this Metaheuristic technique to get optimum pi controller gains for rotor and grid side of wind turbines to improve its LVRT capability as said by grid code requirements in abnormal condition.

**A. MOUNTAIN GAZELLE OPTIMIZATION(MGO)**

The Mountain gazelle optimization (MGO) algorithm is a Metaheuristic algorithm influenced by the social hierarchies and levels of trophic activity of mountain gazelles in the wild. The algorithm uses mathematical formulations to simulate the social behavior of gazelles and has been utilized to improve an optimization algorithm. MGO uses four different mechanisms to balance optimization’s exploration and exploitation components. These mechanisms are not specified in the statement but have been designed to achieve a perfect balance in all optimization stages. Finally, MGO has successfully addressed global optimization issues in diverse engineering challenges with high complexity and dimensions. This shows that MGO is a robust and successful optimization method that may be used to solve a broad spectrum of optimization issues in engineering and other industries [43], [44]. The upcoming sections provide the steps used to update the gazelles’ positions, and the equations

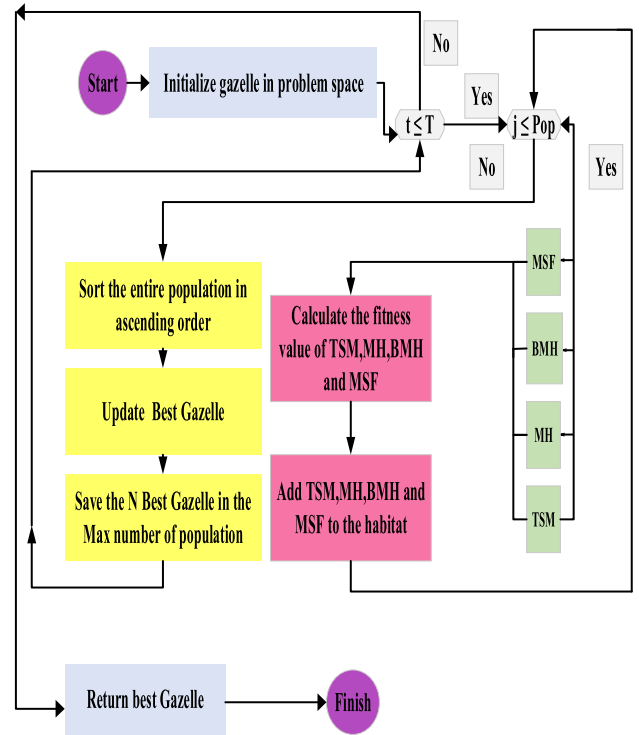


**FIGURE 4. MGO flow chart.**

used to update the gazelles’ positions can be summarized in Figure 4.

**B. MGO MATHEMATICAL MODEL**

The social nature of mountain gazelles prompted the MGO optimization algorithm and how it incorporates different factors from their lives into its optimization process. MGO uses four essential aspects of mountain gazelle daily life: Territory solitary males (TSM), maternal herds, bachelor’s male herds, and foraging behavior. Each gazelle in a procedure may be a member of one of these groups and can potentially give birth to a new gazelle. The most effective global explanation in MGO is a mature male gazelle in a flock habitat. This suggests that the procedure uses a hierarchical structure to organize the optimization process. Finally, MGO performs exploration and exploitation phases in parallel using four different mechanisms [44].

**1) TERRITORIAL SOLITARY MALES (TSM)**

The MGO algorithm includes a mechanism called TSM, which simulates the behavior of male mountain gazelles who create solitary territories and protect them from teens attempting to take parts or females. The TSM mechanism is formulated mathematically using Equation (14), wherein male\_gazelle is a position vector of the optimal global solution (adult male), ri1 and ri2 are arbitrary numbers with values of 1 or 2. Equation (15) is used to compute the youthful male herds factor (BH), F is a factor that can be calculated using Equation (16), and Cof<sub>r</sub> is a chosen coefficient vector that randomness used to improve search capabilities, updated in

each iteration, and computed using Equation (17) [44].

$$TSM = male_{gazelle} | (ri_1 * BH - ri_2 * X(t)) * F | * Cof_r \quad (14)$$

$$BH = X_{ra} - |ri_1| + M_{pr} * |ri_2|, r_a = \left\lfloor \frac{N}{3} \dots \dots \dots N \right\rfloor \quad (15)$$

$$F = N_1(D) * \exp[2 - Iter * \left( \frac{2}{MaxIter} \right)] \quad (16)$$

$$Cof_i = \begin{cases} (a+1) + r_3 \\ (a * N_2 * D) \\ r_4 * (D) \\ (N_3 D * N_4 D^2 * \cos(r_4 * 2) * N_3 D), \end{cases} \quad (17)$$

$$a = -1 + Iter * \left( \frac{-1}{MaxIter} \right) \quad (18)$$

Equation (13), Xra is a randomized choice during the period of ra, M<sub>pr</sub> is the average number of investigators chosen at random [N/3], and N Is the aggregate amount of gazelles, which are. In Equation (16), N1(D) is an arbitrary number selected from the normal distribution, and Iter is the latest iteration value. In Equation (17), a is premeditated using Equation (16), r3 and r4 are arbitrary values between 0 and 1, and N2, N3, and N4 are the size of the issue and integers that vary in the norm range. Finally, in Equation (18), A Is calculated using the existing numeral of iterations (Iter) and the whole sum of repetitions (Maxiter) [44].

2) MATERNITY HERDS (MH)

In Equation (16), the maternity herd mechanism is represented. Here, BH is the scalar of the male youth impact factor derived using Equation (12). Cof<sub>1,r</sub> and Cof<sub>2,r</sub> are coefficient vectors chosen randomly and computed by applying Equation (14). (ri<sub>3</sub> and ri<sub>4</sub> are integers and an arbitrary number of one or two. In the present repetition male<sub>gazelle</sub> is the most suitable (adult male) global answer. Finally, X<sub>rand</sub> represents the vector location of a gazelle chosen randomly from the group of gazelles [44].

$$MH = (BH + Cof_{1,r}) + (ri_3 * male_{gazelle} - ri_4 * X_{rand}) * Cof_{1,r} \quad (19)$$

The Equation represents the movement of the maternity herd in search of food or a better habitat. The first term represents the impact factor of young males on the maternity herd’s movement, while the second term highlights the movement’s effect on local and global optimal solutions. The coefficient vectors Cof<sub>1,r</sub> and Cof<sub>2,r</sub> are used to control the search capability of the algorithm in each iteration [44].

3) BACHELOR MALES HERDS (BMH)

In the Bachelor Male Herds behavior, Equation (20) is used to compute the latest location of a gazelle vector in the present repetition. The new position is obtained by subtracting a distance value D from the current position X(t) and adding a term that depends on the impact factor of young males BH, the best solution male<sub>gazelle</sub>, and two randomly selected

coefficients ri<sub>5</sub> and ri<sub>6</sub>.

$$BMH = (X(t) - D) + (ri_5 * male_{gazelle} - ri_6) * BH * Cof_r \quad (20)$$

The distance value D is calculated using Equation (21), which takes the absolute values of X(t) and male<sub>gazelle</sub>, multiplies them by a random number that can be either -1 or 1, and then sums them [44].

$$D = (/X(t) / + /male_{gazelle} /) * (2 * r_6 - 1) \quad (21)$$

The coefficients Cof<sub>r</sub>, ri<sub>5</sub>, and ri<sub>6</sub> are randomly selected at each iteration, and the most effective solution male<sub>gazelle</sub> is updated as the optimum global position found so far. This behavior represents the movement of bachelor males, who are not part of any herd and may move alone or in small groups.

4) MOVEMENT TO SEARCH FOR FOODS (MSF)

In Equation (22), the variable MSF represents the position of the mountain gazelle after migration. The Equation generates a random number across the issue in the domain’s highest and lowest boundaries, which is added to the gazelle’s current position to simulate the gazelle’s movement in searching for food sources. The parameter r7 is a random integer between 0 and 1, which adds randomness to the migration process. This mechanism ensures that the gazelles can explore various places to discover ideal food sources and prevent excessive grazing in a particular zone [44].

$$MSF = (ub - lb) * r_7 + lb \quad (22)$$

C. GENETIC ALGORITHMS (GA)

The optimization process issues are classified as confined or unconstrained. The concerns are mostly related to the natural evolution processes. The GA periodically updates the population of specific solutions. At each phase, GA selects individuals at random. The chosen individuals are viewed as parents who are used to preparing their offspring for future steps or generations. A population evolves, and an ideal solution is derived from these future generations. Figure 5 depicts the whole process. The algorithm demonstrates that the fundamental mechanisms for determining fitness are selecting, combinations, and mutations (SCM). Table 2 illustrates the GA-based controller gain [45].

D. PARTICLE SWARM OPTIMIZATION (PSO)

Kennedy (1995) introduced the population optimization method (PSO). This technique may produce high-quality solutions in less time and with more reliable converging characteristics than other stochastic approaches such as GA (Cengiz 2011). The method relies on simulations of animal social interactions like fish schooling, bird flocking, and swarming theories. Because it is based on optimal populations and self-adapting, it became a viable alternative to GAs in addressing optimization issues. Figure 6 shows a PSO-based technique to find the ultimate global value for an objective function. The controller PI uses is an excellent

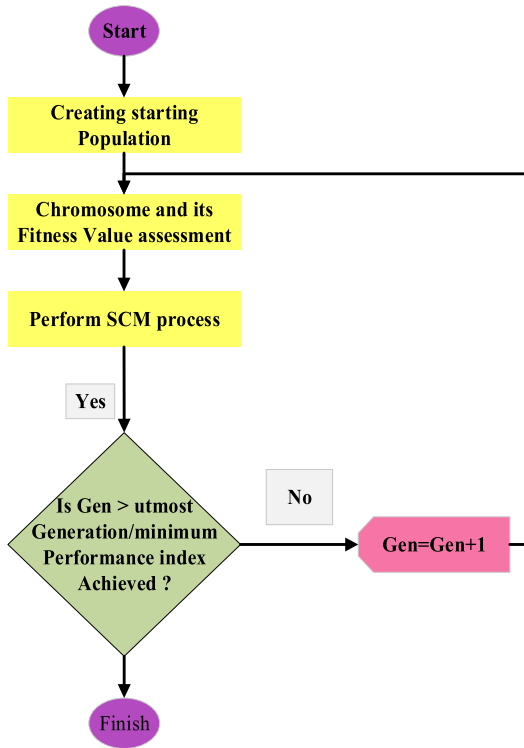


FIGURE 5. GA flow chart.

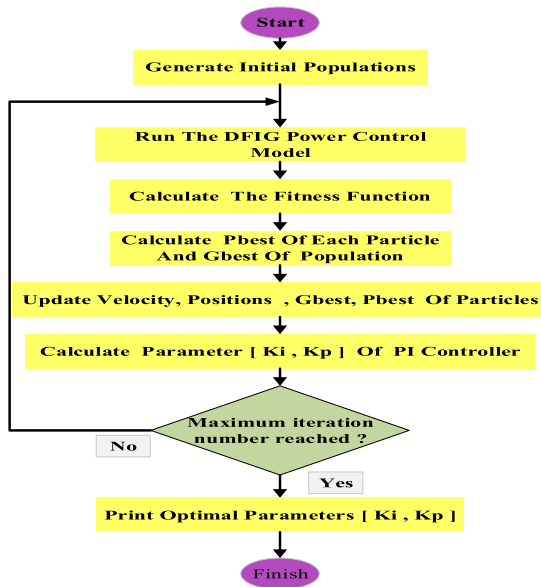


FIGURE 6. PSO flow chart.

machine automation system but requires knowledge of the plant’s mathematical model. Several approaches for tweaking the PI controller have been devised to tackle difficulties in the overall systems. The algorithm as a whole is presented in Figure 6 [46].

**IV. TEST SCENARIOS AND SIMULATION RESULTS**

A typical DFIG wind farm SIMULINK representation has been presented in Figure 1. DFIG is connected with a VSWT and 15 m/s wind speed in the MATLAB/Simulink model.

TABLE 2. Algorithms-based controller gains.

Controller	Grid side current regulator		Rotor side current regulator	
	$k_p$	$k_i$	$k_p$	$k_i$
Gain of the GA	46.5288	67.9453	40.923	125.996
Gain of the PSO	8.16279	92.923	82.6076	100.3676
Gain of the MGO	4.33273	1	20.8195	52.959
Controller	Voltage regulator		DC bus regulator	
	$k_p$	$k_i$	$k_p$	$k_i$
Gain of the GA	16.172	194.933	1.1800	175.812
Gain of the PSO	15.3201	119.173	1	148.803
Gain of the MGO	13.1624	195.84	1.5243	199.183

TABLE 3. DFIG Scheme data set points.

WT Speed	Synchronized DC Voltage	P & Q Power Consideration	Time
1.2 p.u	1 p.u.	1 Pu & 0 MVar	1 s

A wind farm with 9 MW generation is chosen, incorporating six 1.5 MW WT’s. The wind farm is coupled with a 25 kV delivery scheme that carries 120 kV electrical power to the network through a 30 km transmission Line and a 25 kV feeder. A short circuit is applied at the fault point under various unbalanced conditions from 0 s to 0.1 s (6 cycles). Installed circuit breakers will trip to fix the issue in 0.1 s. due to this fault, a disruption voltage sag happens at the DFIG bus voltage. To manage this disruption, the proposed control system is implemented. This control arrangement maintains DC voltages and reactive power to their fixed points, as mentioned in Table 3.

Various simulation tests have been run to investigate the system and compare the proposed controllers effectively. Algorithms were applied to get optimal algorithms-based controller gains [Kp, Ki] for VSWT-DFIG controllers like [Grid side current regulator, Rotor side current regulator, Voltage regulator, and DC bus regulator]. The Metaheuristic technique is tested with a novel algorithm and compared with two traditional criteria by varying the fault type in the proposed system throughout four scenarios. Figure 7 represents the three different convergence curves of MGO, PSO, and GA for DFIG-VSWT. Table 2 shows the recommended settings for MGO and the other two traditional techniques. The Appendix contains a list of DFIG and the turbine parameters utilized in the simulation. Time domain analysis of the recommended DFIG system model with the proposed three techniques has been shown in Figures 8 to 11. Parameters for the time domain (Rising Time, Settling Time, and Maximum Overshoot) and comparative analysis among the three proposed controllers is presented in Tables 4 to 7.



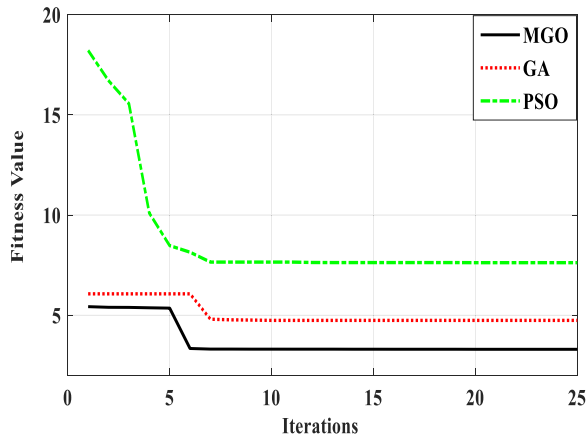


FIGURE 7. Convergence curves of MGO, PSO, and GA for DFIG-VSWT.

TABLE 4. Time domain parameters comparative analysis during a 3-phase voltage unbalance.

Controllers	Rise Time(s)	Settling Time(s)	Peak
MGO-based controller	0.2035	0.1862	1.0839
PSO-based controller	0.2499	0.2311	1.0922
GA-based controller	0.3722	0.3719	1.0885

**A. SCENARIO (1): DFIG DURING A 3-PHASE VOLTAGE UNBALANCE**

simulation results of DFIG schemes during a 3-phase voltage unbalance are shown in Figure 8. Table 4 represents a comparative analysis of time domain parameters among the three proposed controllers.

The simulation findings of MGO are contrasted to GA and PSO for adjusting PI gains. Figure 8 and Table 4 show the DC voltage plus the terminal AC voltage connected to the grid. MGO yields excellent performance and a high reduction in settling time, oscillation, and peak overshoot. Using the innovative MGO algorithm, peak overshoot is reduced by 76% and 42% compared to PSO and GA, respectively. When considering settling time, MGO achieves the best result by lowering it by 99% more than GA and 24% more than PSO. On the other hand, MGO enhances rising time with 22% and 82% compared with PSO and GA, respectively. Many transients with high oscillation and fluctuations appear in GA results during the fault period. MGO aids the DC link voltage and AC voltage in reaching the pre-fault value with minor variation, undershoot, and overshoot. AC voltage has a modest error in steady-state and takes some time to settle. MGO came in the top position for improving DC link voltage and AC voltage, followed by GA in second and PSO in third place.

**B. SCENARIO (2): DFIG DURING A DOUBLE-LINE TO GROUND FAULT**

The Simulation results of DFIG schemes during a double line to ground fault are presented in Figure 9. Table 5 denotes a comparative analysis of time domain parameters among the three proposed approaches.

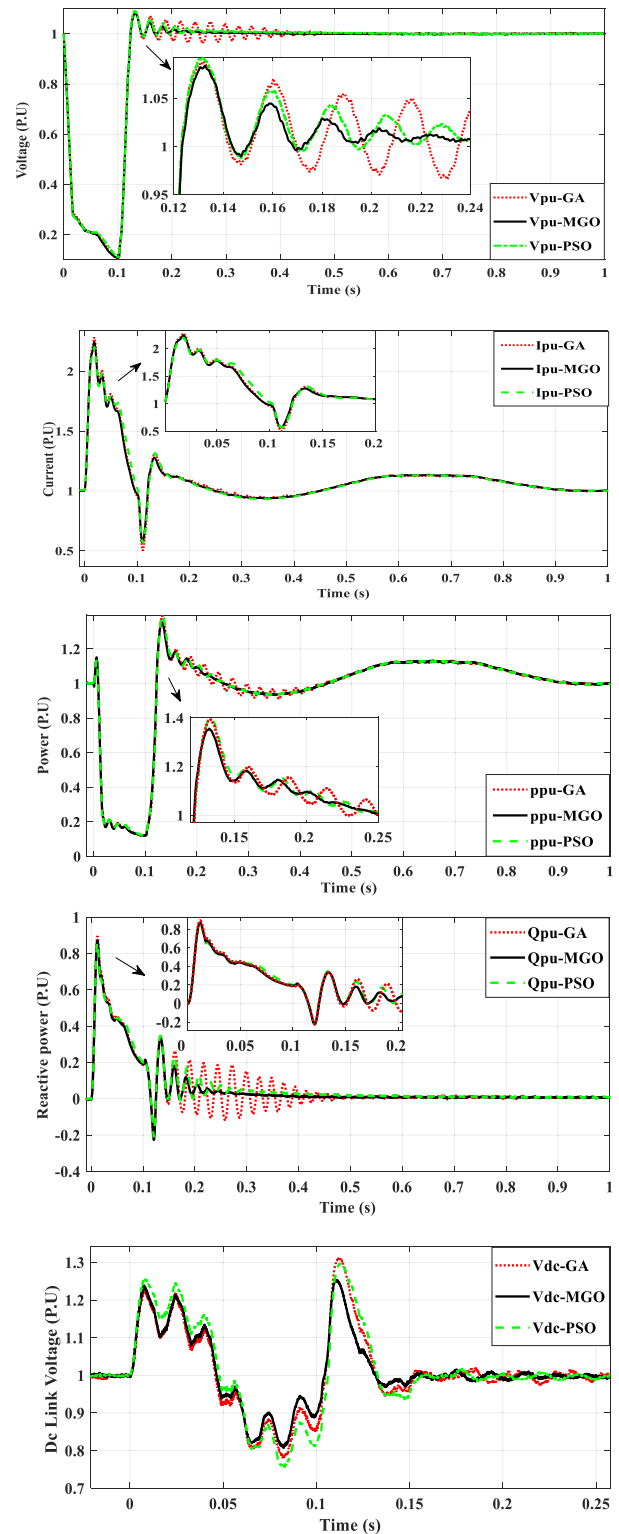


FIGURE 8. DFIG schemes during a 3-phase voltage unbalance.

The MGO technique minimizes the time required for settling the DC link voltage, maximum overshoot, and oscillation. Still, a high range of fluctuations appears in GA results during the fault period. MGO reduced peak overshoot by 71%

**TABLE 5.** Time domain parameters comparative analysis during a double-line to ground fault.

Controllers	Rise Time(s)	Settling Time(s)	Peak
MGO-based controller	0.2513	0.2052	1.0795
PSO-based controller	0.3341	0.2545	1.0796
GA-based controller	0.5044	0.4509	1.0872

**TABLE 6.** Time domain parameters comparative analysis during a line-to-line fault.

Controllers	Rise Time(s)	Settling Time(s)	Peak
MGO-based controller	0.2468	0.2016	1.0816
PSO-based controller	0.3459	0.2570	1.0779
GA-based controller	0.5449	0.4778	1.0789

more than GA and 2% more than PSO, and MGO enhanced settling time by more than 24% and 119% compared with PSO and GA, respectively. From a rising time view, MGO improves it by 32% and 100% compared with PSO and GA, respectively. MGO is still in the top position for improving DC link voltage and AC voltage, but PSO is in second position, followed by GA in third place.

**C. SCENARIO (3): DFIG DURING A LINE -TO- LINE FAULT**

Simulation results of DFIG schemes during a line-to-line fault (unbalance) are exposed in Figure 10. Table 6 represents a comparative analysis of time domain parameters among the three proposed techniques.

The identical wind system parameters are used in this case; however, a line-to-line fault is generated to test performances under various circumstances. Figure 10 and Table 6 demonstrate that modifying the PI controller via MGO outperforms the alternative metaheuristic method. MGO outperforms PSO and GA by lowering settling time and fluctuation. Maximum overshoot is decreased by 34% and 25% compared with PSO and GA, respectively. In the instance of MGO, notice that AC voltage achieved by utilizing MGO in PI gain adjustment improved transient stability and settling time by 27% over PSO and 137% over GA. Also, MGO is better than PSO and GA, with 40% and 120%, respectively. MGO enhances settling time and reaches per-unit value faster and better than conventional techniques. GA is still in the high oscillation range in period fault and tries to reach a stable value again.

**D. SCENARIO (4): DFIG DURING A LINE TO GROUND FAULT**

Simulation results of DFIG schemes during a line-to-ground fault (unbalanced) are revealed in Figure 11. Table 7

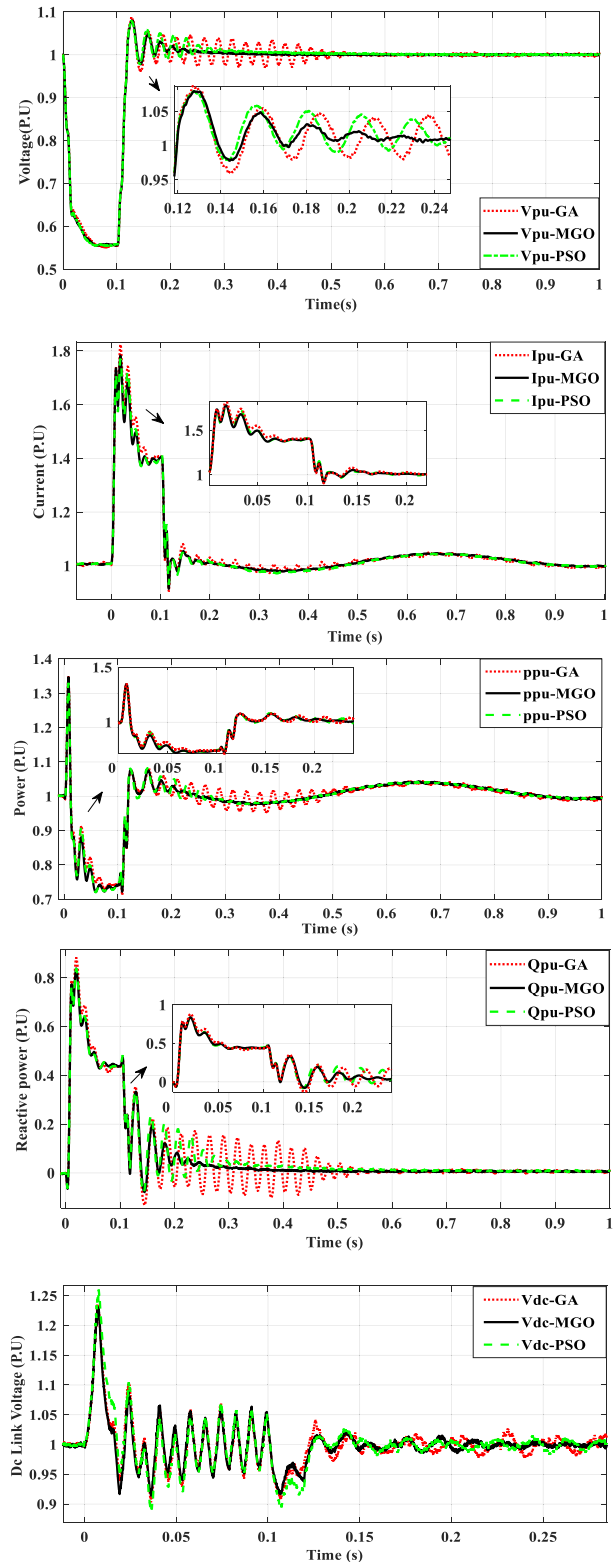


**FIGURE 9.** DFIG schemes during a double -line to ground fault.

represents a comparative analysis of time domain parameters among the three proposed controllers.

All wind framework parameter settings remain unchanged from the preceding scenario. Figure 11 and Table 7 indicate

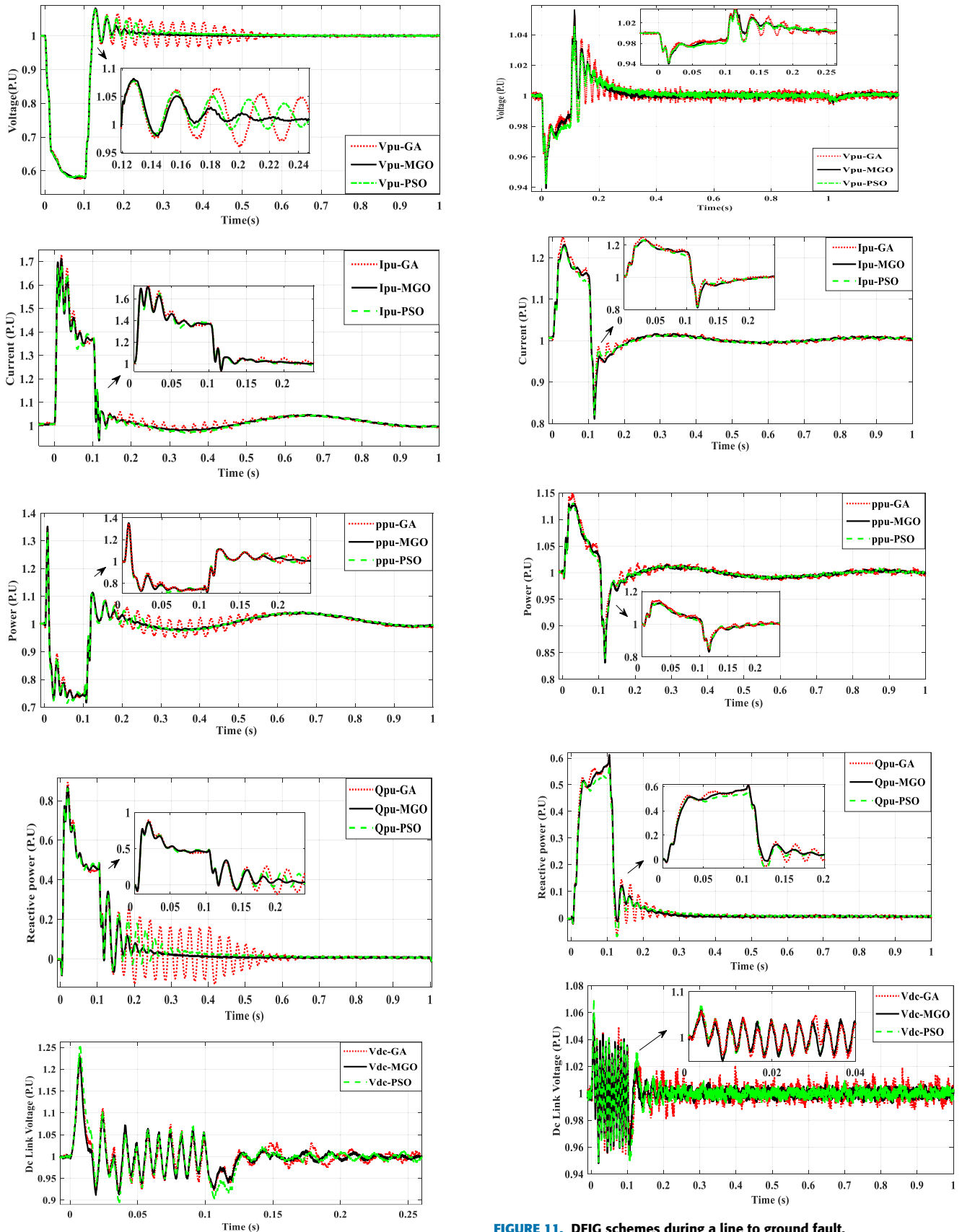


FIGURE 11. DFIG schemes during a line to ground fault.

FIGURE 10. DFIG schemes during a line-to-line fault.

**TABLE 7. Time domain parameters comparative analysis during a line to ground fault.**

Controllers	Rise Time(s)	Settling Time(s)	Peak
MGO-based controller	0.2075	0.1640	1.0460
PSO-based controller	0.2198	0.1670	1.0563
GA-based controller	0.2497	0.1876	1.0528

that utilizing MGO to tune PI gains decreased the maximum overshoot point by 0.98% and 0.65% compared with GA and PSO, respectively. MGO reduces settling time by 1.8% compared to PSO and with a 14% contract with GA. From a rising time view, MGO enhances it by 6%,20% compared with PSO and GA. MGO provides better-damped performance, reduced steady-state error, and fast settling time and variations. MGO helps DC link and AC voltage approach a pre-fault value faster than any other method. The innovative meta-heuristic algorithm MGO can enhance grid-dependent wind turbines' operational efficiency during various failures with improved responses.

**V. CONCLUSION**

This paper addressed the optimal control strategies for enhancing the Low Voltage Ride Through (LVRT) capability of grid-tied wind power stations and presented the significance of optimal control strategy for improving the LVRT capability of grid-tied wind power stations. The conducted research demonstrated an ideal PI controller adjusting for a 9-MW DFIG grid-connected wind power system. This paper proposed an innovative design technique of MGO-based optimal PI controllers in grid-connected wind power systems' RSC or GSC converter to enhance LVRT capability. The system's responsiveness for the wind system under the proposed control system exceeded grid code requirements for increasing the LVRT capabilities when subjected to symmetric and unsymmetrical fault scenarios. The effectiveness of the simulated optimization technique is established by comparing its results to those produced using conventional PSO and GA. With the suggested MGO, this approach enhanced system performance, such as (less computing time, reduced overshoot, and better settling time with less steady-state error). The proposed novel optimization method produced satisfactory results, demonstrating that these gain controller solutions are ideal for symmetrical and unsymmetrical stator voltage drops. The proposed controllers were revealed to be faster, with fewer fluctuations, and better damping than conventional techniques. For instance, the outcomes of the first investigated case (a 3-Phase Voltage Unbalance) show that utilizing the MGO reduced peak overvoltage by 76% and 42% compared with PSO and GA, respectively. In the second case (a Double-Line to Ground Fault), results prove that MGO has reduced peak overshoot by 71% more than GA and 2% more than PSO. In the third case (a Line-to-Line Fault) and the presence of MGO, voltage overshoot

was reduced by 34%, and settling time was enhanced by more than 27% compared with PSO. Finally, in the last case (a Line to Ground Fault), MGO reduced settling time by a high value of more than 14% and 1.8% compared with GA and PSO, respectively. Overall, the results confirmed that the proposed technique achieved the best optimal results when constructed to traditional alternative algorithms-based PI controllers. Demonstrating the viability of the recommended control approach. Finally, we conclude that the MGO-based PI control technique successfully improved the LVRT capabilities of wind systems compared to traditional PSO and GA techniques.

In future works, artificial intelligent neural network-based adaptive management for a DFIG-based the WECS with additional devices might be a strong choice.

**APPENDIX A**

**A.1 DFIG PARAMETERS**

Variable	Value
Rated Power (Pm)	9 MW
Stator resistance (Rs)	0.0092 Ω
Rotor resistance (Rr)	0.0076 Ω
Pole Pairs (p)	2
Stator inductance (Ls)	0.19 H
Rotor inductance (Lr)	0.0792 H
Mutual inductance (Lm)	4.5926 H
The friction coefficient (f)	0.0024 N.m. s-1
Slip (g)	0.03
The angular speed (s)	157 d/s

**A.2 TURBINE PARAMETERS**

Variable	Value
Radius of the wind	35.25 m
Air density	1.225/m3

**A.3 FEED PARAMETERS**

Variable	Value
Stator rated voltage (Vs)	25/ 120 kV
Rated frequency stator (fs)	50 HZ
Rotor rated voltage (fr)	575 V/ 25 kV
Rated frequency stator (Vr)	14 Hz

**ACKNOWLEDGMENT**

This work was supported by the Researchers Supporting Project number (RSP2023R258), King Saud University, Riyadh, Saudi Arabia.

## REFERENCES

- [1] R. Tiwari and N. R. Babu, "Recent developments of control strategies for wind energy conversion system," *Renew. Sustain. Energy Rev.*, vol. 66, pp. 268–285, Dec. 2016.
- [2] R. A. Turky, T. S. Abdelsalam, H. M. Hasanien, M. Alharbi, Z. Ullah, S. M. Muyeen, and A. M. Abdeen, "Adaptive controlled superconducting magnetic energy storage devices for performance enhancement of wind energy systems," *Ain Shams Eng. J.*, vol. 14, no. 7, Jul. 2023, Art. no. 102343.
- [3] E. Strantzali and K. Aravossis, "Decision making in renewable energy investments: A review," *Renew. Sustain. Energy Rev.*, vol. 55, pp. 885–898, Mar. 2016.
- [4] O. P. Bharti, R. K. Saket, and S. K. Nagar, "Controller design for DFIG driven by variable speed wind turbine using static output feedback technique," *IEEE Access*, vol. 6, pp. 1056–1061, 2016.
- [5] O. Pfeiffer, D. Nock, and A. Baker, "Wind energy's bycatch: Offshore wind deployment impacts on hydro power operation and migratory fish," *Renew. Sustain. Energy Rev.*, vol. 143, Jun. 2021, Art. no. 110885.
- [6] M. Abdulrahman and D. Wood, "Wind farm layout upgrade optimization," *Energies*, vol. 12, no. 13, p. 2465, Jun. 2019.
- [7] S. S. Sahoo, A. Roy, and K. Chatterjee, "Fault ride through enhancement of wind energy conversion system adopting a mechanical controller," *Appl. Sci.*, vol. 143, pp. 110885–110900, Jun. 2016.
- [8] H. Torkaman and A. Keyhani, "A review of design consideration for doubly fed induction generator based wind energy system," *Electric Power Syst. Res.*, vol. 160, pp. 128–141, Jul. 2018.
- [9] F. Gebru, B. Khan, and H. H. Alhelou, "Analyzing low voltage ride through capability of doubly fed induction generator based wind turbine," *Energy Convers. Manage.*, vol. 86, pp. 1785–1795, May 2020.
- [10] N. K. Mishra and Z. Husain, "Application of novel six phase doubly fed induction generator for open phases through modeling and simulation," *ISA Trans.*, vol. 67, pp. 210–218, Aug. 2021.
- [11] Y. Belgaid, M. Helaimi, R. Taleb, and M. B. Youcef, "Optimal tuning of PI controller using genetic algorithm for wind turbine application," *IEEE Access*, vol. 18, pp. 167–178, 2020.
- [12] E. El Hawatt, M. S. Hamad, and K. H. Ahmed, "Low-voltage ride-through capability enhancement of a DFIG wind turbine using a dynamic voltage restorer with Adaptive Fuzzy PI controller," *Electr. Power Syst. Res.*, July 2013, Vol. 143, pp. 110885–110890.
- [13] M. H. Qais, H. M. Hasanien, and S. Alghuwainem, "Optimal transient search algorithm-based PI controllers for enhancing low voltage ride-through ability of grid-linked PMSG-based wind turbine," *Electronics*, vol. 9, no. 11, pp. 1807–1820, Oct. 2020.
- [14] J. Vidal, G. Abad, J. Arza, and S. Aurtenechea, "Single-phase DC crowbar topologies for low voltage ride through fulfillment of high-power doubly fed induction generator-based wind turbines," *IEEE Trans. Energy Convers.*, vol. 28, no. 3, pp. 768–781, Sep. 2013.
- [15] K. Reddy and A. Saha, "A heuristic approach to optimal crowbar setting and low voltage ride through of a doubly fed induction generator," *Energy Convers. Manage.*, vol. 56, pp. 9300–9307, Apr. 2022.
- [16] M. Elsisli, M.-Q. Tran, K. Mahmoud, M. Lehtonen, and M. M. F. Darwish, "Robust design of ANFIS-based blade pitch controller for wind energy conversion systems against wind speed fluctuations," *IEEE Trans.*, vol. 56, no. 9, pp. 37894–37904, Jul. 2021.
- [17] N. H. Saad, A. A. El-Sattar, and M. E. Marei, "Improved bacterial foraging optimization for grid connected wind energy conversion system based PMSG with matrix converter," *Ain Shams Eng. J.*, vol. 9, no. 4, pp. 2183–2193, Dec. 2018.
- [18] M. Nasiri and A. Arzani, "Robust control scheme for the braking chopper of PMSG-based wind turbines—A comparative assessment," *Int. J. Electric Power Energy Syst.*, vol. 134, pp. 107–113, Jan. 2022.
- [19] M. A. S. Ali, K. K. Mehmood, S. Baloch, and C.-H. Kim, "Modified rotor-side converter control design for improving the LVRT capability of a DFIG-based WECS," *Electric Power Syst. Res.*, vol. 186, Sep. 2020, Art. no. 106403.
- [20] F. E. V. Taveiros, L. S. Barros, and F. B. Costa, "Heightened state-feedback predictive control for DFIG-based wind turbines to enhance its LVRT performance," *Int. J. Electr. Power Energy Syst.*, vol. 104, no. 11, pp. 943–956, 2019.
- [21] S. Mali, S. James, and I. Tank, "Improving low voltage ride-through capabilities for grid connected wind turbine generator," *Energy Proc.*, vol. 54, pp. 530–540, 2014.
- [22] N. A. Mohamed, H. M. Hasanien, E. A. Al-Ammar, M. Tostado-Véliz, R. A. Turky, F. Jurado, and A. O. Badr, "Gorilla tropical optimization algorithm solution for performance enhancement of offshore wind farm," *IET Gener., Transmiss. Distribution*, vol. 17, no. 10, pp. 2388–2400, May 2023.
- [23] M. Muyeen and A. Al-Durra, "Modeling and control strategies of fuzzy logic-controlled inverter system for grid interconnected variable speed wind generator," *Energies*, vol. 7, pp. 817–824, Feb. 2013.
- [24] N. A. Mohamed, H. M. Hasanien, A. Alkuhayli, T. Akmaral, F. Jurado, and A. Badr, "Hybrid particle swarm and gravitational search algorithm-based optimal fractional order PID control scheme for performance enhancement of offshore wind farms," *Sustainability*, vol. 15, pp. 11912–11920, Aug. 2023.
- [25] Z. Abdmouleh, A. Gastli, L. Ben-Brahim, M. Haouari, and N. A. Al-Emadi, "Review of optimization techniques applied for the integration of distributed generation from renewable energy sources," *Appl. Energy*, vol. 113, pp. 266–280, Dec. 2017.
- [26] Y. Tang, B. Wei, X. Xia, and L. Gui, "Dynamic multi-swarm particle swarm optimization based on learning," *IEEE Trans.*, vol. 7, no. 4, pp. 184–195, Jun. 2019.
- [27] H. Bakir, A. Merabet, R. K. Dhar, and A. A. Kulaksiz, "Bacteria foraging optimization algorithm based optimal control for doubly-fed induction generator wind energy system," *Int. J. Electr. Power Energy Syst.*, vol. 14, pp. 1850–1859, 2020.
- [28] J. Wang, C. Liu, and M. Zhu, "Improved bacterial foraging algorithm for cell formation and product scheduling considering learning and forgetting factors in cellular manufacturing systems," *IEEE Trans.*, vol. 14, pp. 3047–3056, 2020.
- [29] L. F. Zhu, J. S. Wang, H. Y. Wang, S. S. Guo, and M. W. Guo, "Data clustering method based on improved bat algorithm with six convergence factors and local search operators," *ISA Trans.*, vol. 8, pp. 80536–80560, Aug. 2020.
- [30] E. E. Elattar and S. K. E. Sayed, "Optimal location and sizing of distributed generators based on renewable energy sources using modified moth flame optimization technique," *IEEE Access*, vol. 78, pp. 109625–109638, 2020.
- [31] L. Hongwei, L. Jianyong, C. Liang, B. Jingbo, S. Yangyang, and L. Kai, "Chaos-enhanced moth-flame optimization algorithm for global optimization," *J. Syst. Eng. Electron.*, vol. 30, no. 6, pp. 1144–1159, Dec. 2019.
- [32] P. C. Krause, O. Wasynczuk, and S. D. Sudoff, "Analysis of electric machinery and drive systems," *Energy Convers. Manage.*, vol. 78, no. 4, pp. 88–95, 2014.
- [33] T. Magesh, G. K. Sandhia, J. Ramaprabha, and G. Devid, "Golden eagle optimization algorithm based on a PI control scheme to enhance the dynamic stability of a wind turbine with a double-fed induction generator," *Int. J. Eng. Syst.*, vol. 2, pp. 88–95, 2023.
- [34] J. M. A. Mostafa, E. A. El-Hay, and M. M. Elkholi, "Optimal low voltage ride-through of wind turbine doubly fed induction generator based on bonobo optimization algorithm," *Appl. Energy*, vol. 13, no. 4, pp. 770–777, 2023.
- [35] S. Yamparala, L. L. Arasimman, and G. Sambasiva, "Improvement of LVRT capability for DFIG based WECS by optimal design of FoPID controller using SLNO + GWO algorithm," *Int. J. Eng. Syst.*, vol. 1, pp. 202–213, Jan. 2023.
- [36] A. Tilli, C. Conficoni, and A. Hashemi, "An effective control solution for doubly-fed induction generator under harsh balanced and unbalanced voltage sags," *Electric Power Syst. Res.*, vol. 84, no. 4, pp. 172–182, 2019.
- [37] M. F. El-Naggar, M. I. Mosaad, H. M. Hasanien, T. A. AbdulFattah, and A. F. Bendary, "Elephant herding algorithm-based optimal PI controller for LVRT enhancement of wind energy conversion systems," *Ain Shams Eng. J.*, vol. 12, no. 1, pp. 599–608, Mar. 2021.
- [38] R. Hiremath and T. Moger, "Modified super twisting algorithm based sliding mode control for LVRT enhancement of DFIG driven wind system," *Int. J. Eng. Syst.*, vol. 8, no. 4, pp. 3600–3613, 2012.
- [39] O. P. Bharti, R. K. Saket, and S. Nagar, "Controller design for DFIG driven by variable speed wind turbine using soft computational techniques," *IEEE Access*, vol. 6, pp. 1056–1061, 2016.
- [40] B. Hamanea, M. Benganemb, A. M. Bouzid, A. Belaabes, and M. Bouhamid, "Control for variable speed wind turbine driving a doubly fed induction generator using fuzzy-PI control," *Appl. Energy*, vol. 18, pp. 476–485, Sep. 2012.
- [41] K. E. Okedu, M. A. S. A. Tobi, and S. Alaraimi, "Comparative study of the effects of machine parameters on DFIG and PMSG variable speed wind turbines during grid fault," *Electric Power Syst. Res.*, vol. 70, pp. 643–658, May 2021.

- [42] L. Zhang, C. Watthansarn, and W. Shehered, "A matrix converter excited doubly-fed induction machine as a wind power generator," in *Proc. 7th Int. Conf. Power Electron. Variable Speed Drives*, vol. 2, Sep. 2018, pp. 532–537.
- [43] B. Abdollahzadeh, F. S. Gharehchopogh, N. Khodadadi, and S. Mirjalili, "Mountain gazelle optimizer: A new nature-inspired metaheuristic algorithm for global optimization problems," *Adv. Eng. Softw.*, vol. 174, Oct. 2022, Art. no. 103282.
- [44] P. R. Sahoo, J. K. Goyal, S. Ghosh, and A. K. Naskar, "New results on restricted static output feedback H controller design with regional pole placement," *ISA Trans.*, vol. 13, no. 8, pp. 95–104, 2019.
- [45] A. Feijóo, J. Cidrás, and C. Carrillo, "A third order model for the doubly-fed induction machine," *Electric Power Syst. Res.*, vol. 56, no. 2, pp. 121–130, Nov. 2000.
- [46] Y. Bekakra and D. B. Attous, "Optimal tuning of PI controller using PSO optimization for indirect power control for DFIG based wind turbine with MPPT," *Int. J. Electr. Power Energy Syst.*, vol. 24, no. 4, pp. 890–898, 2014.



dynamics and control, energy storage systems, renewable energy systems, and smart grids.

**FATMA EL ZAHRAA MAGDY** received the B.Sc. degree in electrical power engineering from Science Valley Academy, in 2017, and the M.Sc. degree in electrical power engineering from the Faculty of Engineering, Cairo University, Cairo, Egypt, in 2020. She is currently pursuing the Ph.D. degree with Ain Shams University. She has published more than three papers in international journals and conferences. Her research interests include modern control techniques, power systems



currently a Professor with the Department of Electrical Power and Machines, Faculty of Engineering, Ain Shams University. His research interests include modern control techniques, power systems dynamics and control, energy storage systems, renewable energy systems, and smart grids. He is an Editorial Board Member of *Electric Power Components and Systems*. He is a Subject Editor of *IET Renewable Power Generation*, *Frontiers in Energy Research*, and *Electronics* (MDPI). He has authored, coauthored, and edited three books in the field of electric machines and renewable energy. He has published more than 250 papers in international journals and conferences. His biography has been included in Marquis Who's Who in the World for its 28th Edition, in 2011. He was awarded the Encouraging Egypt Award for Engineering Sciences, in 2012. He was awarded the Institutions Egypt Award for Invention and Innovation of Renewable Energy Systems Development, in 2014. He was awarded the Superiority Egypt Award for Engineering Sciences, in 2019. He was the IEEE PES Egypt Chapter Chair, from 2020 to 2022. He is the Editor-in-Chief of *Ain Shams Engineering Journal* (Elsevier).

**HANY M. HASANIEN** (Senior Member, IEEE) received the B.Sc., M.Sc., and Ph.D. degrees in electrical engineering from the Faculty of Engineering, Ain Shams University, Cairo, Egypt, in 1999, 2004, and 2007, respectively. From 2008 to 2011, he was a Joint Researcher with the Kitami Institute of Technology, Kitami, Japan. From 2012 to 2015, he was an Associate Professor with the College of Engineering, King Saud University, Riyadh, Saudi Arabia. He is



the M.Sc. degree in mathematical statistics from the ISSR, Cairo University,

**WAHEED SABRY** received the B.Sc. degree in electrical engineering from the Department of Electrical Power and Energy, Military Technical College (MTC), Cairo, Egypt, in June 1987, the M.Sc. degree in electrical engineering from MTC, in January 1993, the Diploma degree in statistics from the Institute of Statistical Studies and Researches (ISSR), Cairo University, Cairo, in June 1995, the Ph.D. degree in electrical engineering from MTC, in February 1998, and

in June 2002. In 2001, he joined the Bradley Department of Electrical and Computer Engineering, Virginia Polytechnic Institute and State University (Virginia Tech), Blacksburg, VA, USA, as a Postdoctoral Researcher. He was an Associate Professor of electrical engineering, in January 2005, and a Full Professor of electrical engineering, in January 2015. From June 2001 to January 2011, he was the Head of the Department of Electrical Power and Energy, MTC. Since January 2005, he has been the Head of the Department of Electrical Power and Energy, Scientific Council, MTC. From September 2015 to August 2016, he was the Dean of the High Institute for Engineering and Technology, Luxor, Egypt. From September 2016 to January 2020, he was the Head of the Department of Electrical Power and Energy, Valley Higher Institute for Engineering and Technology, Science Valley Academy (SVA), Cairo. From February 2020 to September 2020, he was a Professor of electrical engineering with the Higher Technological Institute (HTI), 10th of Ramadan City, Sharqia, Egypt. From October 2020 to August 2023, he was the Dean of the High Institute of Engineering and Technology, King Mariout, Alexandria, Egypt. He is currently the Head of the Department of Electrical Engineering, Giza Engineering Institute (GEI), Cairo. His research interest includes power system control and stability.



planning with RES, operation and control, EV integrated distribution networks optimization, EV charging station designing, and EV scheduling optimization.

**ZIA ULLAH** (Member, IEEE) received the Ph.D. degree in electrical engineering from the Huazhong University of Science and Technology (HUST), Wuhan, China, in 2020. He is currently a Postdoctoral Research Fellow with the State Key Laboratory of Advanced Electromagnetic Engineering and Technology, School of Electrical and Electronic Engineering, HUST. His research interests include power system optimization, intelligent power distribution systems, distribution system



Company. He is currently an Assistant Professor with the Department of Electrical Engineering, King Saud University. His research interests include energy management, renewable energy systems, flexible ac transmission systems, power system stability, and smart grids. He was a recipient of the IEEE Electromagnetic Compatibility Society Best Symposium Paper Award, in 2011.

**ABDULAZIZ ALKHAYLI** (Member, IEEE) received the B.Sc. degree in electrical engineering from King Saud University, Riyadh, Saudi Arabia, in 2006, the M.S. degree in electrical engineering from the Missouri University of Science and Technology, Rolla, MO, USA, in 2013, and the Ph.D. degree in electrical engineering from North Carolina State University, Raleigh, NC, USA, in 2018. From 2006 to 2009, he was an Operation Engineer with the Energy Control Center, Saudi Electricity



energy, and electrical power systems analysis, stability, and control.

**AHMED H. YAKOUT** received the B.Sc. and M.Sc. degrees from the Department of Electrical Power and Machines, Faculty of Engineering, Ain Shams University, Cairo, Egypt, in 2000 and 2005, respectively, and the Ph.D. degree in electrical engineering from the University of Strathclyde, Glasgow, U.K., in 2010. He is currently an Associate Professor with the Faculty of Engineering, Ain Shams University. His main research interests include modern control techniques, renewable

...